E_2P Phosphoforms of Na,K-ATPase. II. Interaction of Substrate and Cation-Binding Sites in P_i Phosphorylation of Na,K-ATPase†

Flemming Cornelius,* Natalya U. Fedosova, and Irena Klodos

Department of Biophysics, University of Aarhus, DK-8000 Denmark

Received July 1, 1998; Revised Manuscript Received September 21, 1998

ABSTRACT: In this investigation the effects of alkali cations on the transient kinetics of Na,K-ATPase phosphoenzyme formation from either ATP (E_2P) or P_i (E'_2P) were characterized by chemical quench methods as well as by stopped-flow RH421 fluorescence experiments. By combining the two methods it was possible to characterize the kinetics of Na,K-ATPase from two sources, shark rectal glands and pig kidney. The rate of the spontaneous dephosphorylation of E_2P and E'_2P was identical with a rate constant of about 1.1 s^{-1} at 20 °C. However, whereas dephosphorylation of E_2P formed from ATP was strongly stimulated by K^+, dephosphorylation of E'_2P formed from P_i in the absence of alkali cations was K^+-insensitive, although in pig renal enzyme K^+ binding to E'_2P could be demonstrated with RH421 fluorescence. It appears, therefore, that in pig kidney enzyme the rapid binding of K^+ to E'_2P was followed by a slow transition to a nonfluorescent form. For shark enzyme the K^+-induced decrease of RH421 fluorescence of P_i phosphorylated enzyme was due to K^+ binding to the dephosphoenzyme (E_1), thus shifting the equilibrium away from E'_2P. When P_i phosphorylation was performed with enzyme equilibrated with K^+ or its congeners Tl^+, Rb^+, and Cs^+ but not with Na^+ or Li^+, both the phosphorylation and the dephosphorylation rates were considerably increased. This indicates that binding of cations modifies the substrate site in a cation-specific way, suggesting an allosteric interaction between the conformation of the cation-binding sites and the phosphorylation site of the enzyme.

The phosphoforms formed from ATP or P_i[1] have been regarded as chemically identical (*1*−*8*). However, over the years evidence has accumulated showing that the two phosphoenzyme forms are kinetically different, especially regarding the different K^+ sensitivity of the dephosphorylation reactions as shown by Post et al. (*3*). Post et al. (*3*, *9*) suggested that the observed differences in K^+ sensitivity were due to the binding of a second Mg^{2+} to the MgE_2P phosphoform. More recently, we have shown (*10*) that the two phosphointermediates differ in their interaction with vanadate, in their susceptibility to *N*-methyl hydroxylamine, and in the phosphorylation-induced fluorescence response with the fluorophore RH421. On the basis of these differences a subconformation of the E_2P form with the notation E'_2P was proposed for the phosphoenzyme formed from P_i (*10*). We ascribe the different properties of the two phosphoenzymes to an intrinsic feature of the subconformation E'_2P, implying that the phosphoforms produced by the two routes of phosphorylation differ in the structure of the substrate site which, in turn, induces an altered organization of the cation-binding site.

In the present paper we compare the different kinetic properties of the phosphoenzymes formed from ATP and P_i measured by transient chemical and RH421 fluorescence methods. Fluorescence experiments are advantageous by easily allowing both transient and equilibrium measurements; however, a main problem can be the proper assignment of high- and low-fluorescence levels to known intermediate enzyme forms. In the preceding paper (*10*), we demonstrate that RH421 detects the formation of acid-stable phosphoenzyme formed from P_i (cf. Apell et al. (*11*)), and in the present paper, we show that binding of alkali cations to this phosphoform induces states that are low-fluorescent. Together with the chemical analysis, this enables us to characterize the kinetics of phosphoenzyme formation from P_i in the presence and absence of different alkali cations. We compare two enzyme preparations, shark rectal and pig renal Na,K-ATPase, which has previously been shown to be phosphorylated by P_i to different levels (10).

The cations studied were the following: (1) Na^+ and Li^+ which are known to mainly stabilize the E_1 conformation by shifting the equilibrium, $E_2 \rightarrow E_1 \rightarrow E_1Na_3$; and (2) K^+ and its congeners Rb^+, Tl^+, and Cs^+ which are known to stabilize the E_2 conformation by increasing the rate of the $E_1 \rightarrow E_2(K_2)$ transition.

Preliminary results have previously been presented in abstract form (*12*).

† This work was supported in part by The Danish Research Academy (fellowship to N.U.F.), The Danish Medical Research Council, The Danish Biomembrane Research Centre, University of Aarhus, and the NOVO foundation.

* To whom correspondence should be addressed. Tel: +45 89422937. Fax: +45 86129599. E-mail: fc@biophys.au.dk.

[1] Abbreviations: E_1, Na,K-ATPase form with high affinity toward ATP and Na^+; E_2, Na,K-ATPase form with high affinity toward K^+ and low affinity to ATP; EP, phosphoenzyme; E_1P, ADP-sensitive phosphoenzyme; E_2P, K^+-sensitive phosphoenzyme; E'_2P, K^+-insensitive phosphoenzyme formed from P_i in the absence of monovalent cations; E_2V, enzyme−vanadate complex; P_i, inorganic phosphate; V, vanadate; K_{Pi} and $K_{0.5\ Pi}$, dissociation constant and apparent dissociation constant characterizing binding of P_i; K_K and $K_{0.5\ K}$, dissociation constant and apparent dissociation constant characterizing the interaction with K^+; $K_{0.5}$, the concentrations which yield half-maximum response.

10.1021/bi981571v CCC: $15.00
Published on Web 11/10/1998

EXPERIMENTAL PROCEDURES

Enzyme Preparation. Na,K-ATPase (EC 3.6.1.37) from shark rectal glands and pig kidney was purified as previously described (*13*, *14*, *15*). The specific hydrolytic activity measured at 37 °C and under standard conditions (*16*) was 30−33 units/mg of protein for shark enzyme and about 25 units/mg of protein for pig kidney enzyme. The protein content was determined according to Lowry et al. (*17*), as described by Jensen & Ottolenghi (*18*), using bovine serum albumin as standard.

Phosphorylation. Phosphorylation of Na,K-ATPase from [γ-^{32}P]ATP (10 μM- 1 mM) was performed as previously described by Cornelius (*19*) in a medium containing 4 mM $MgCl_2$, 16 mM NaCl, and 30 mM imidazole, pH 7.4. Phosphorylation of the enzyme from $^{32}P_i$ (1 mM) was performed according to Cornelius (*19*) in 4 mM $MgCl_2$, 10 mM HEPES/10 mM MES, or 30 mM imidazole, pH 7.5.

Dephosphorylation. Dephosphorylation of Na,K-ATPase after ATP phosphorylation was measured by chasing with unlabeled ATP (1 mM) followed by the addition of an acid stopping solution in the presence of 10 mM $MgCl_2$ as previously described (*19*). Dephosphorylation of the phosphoenzyme after P_i phosphorylation (1 mM) was measured either after a fifty times dilution of the ^{32}P or by chasing with 50 mM unlabeled P_i followed by addition of the stopping solution containing 10% trichloracetic acid and 2 mM sodium pyrophosphate. No differences between the two methods were noted. For fast reactions a rapid mixing quenched-flow apparatus was used.

RH421 Fluorescence Measurements. Steady-state and transient RH421 fluorescence was measured as described in the preceding paper (*10*) using 50 μg/mL Na,K-ATPase in the presence of 4 mM $MgCl_2$ in 10 mM HEPES/10 mM MES or in 30 mM imidazole, adjusted with *N*-methyl-D-glucamine to pH 7.5.

Data Analysis. Monoexponential and double-exponential functions were used to fit the phosphorylation and dephosphorylation data. The goodness of the fits was quantified using an F-test and a 5% confidence level. If double-exponential time functions fitted the data significantly better than monoexponential equations the observed rate constants (λ_1, λ_2) and the values for the rapid and slow phases (f_1, f_2) are given. For double-exponential time functions the initial rates were calculated as $v_0 = \lambda_1 f_1 + \lambda_2 f_2$ (*19*). Two points should be emphasized regarding biphasic kinetics: (1) it can result from several different models, not necessarily a two-pool model, and (2) neither the observed rate constants nor the fast and slow phases in such fits can be ascribed to any single rate constant or pool size in a kinetic model (*20*).

The time course of stopped-flow RH421 fluorescence associated with P_i phosphorylation of the enzyme was fitted to model reaction schemes using the program DYNAFIT (*21*).

Materials. ATP, purchased as the sodium salt from Boehringer Mannheim, Germany, was converted to the Tris salt by chromatography on a Dowex 1 column (from Sigma Chemicals Co., St. Louis, MO). γ^{32}P-ATP and $^{32}P_i$ were from Amersham. RH421 was purchased from Molecular Probes, INC, Eugene, OR, and dissolved in dimethyl sulfoxide. *N*-2-Hydroxyethylpiperazine-*N*′-ethanesulfonic acid (HEPES), 2-*N*-morpholinoethanesulfonic acid (MES), and *N*-methyl-D-glucamine were purchased from Sigma. All other reagents were reagent grade.

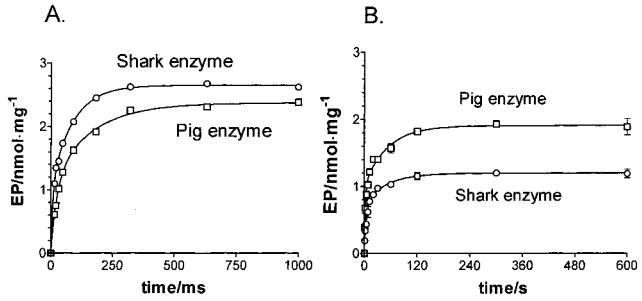

FIGURE 1: Chemical quench measurements of phosphorylation of Na,K-ATPase from pig kidney (□) and shark (○) by [γ-^{32}P]ATP (1 mM) in the presence of 16 mM Na^+ (A) or 1 mM $^{32}P_i$ in the absence of alkali cations (B). All experiments were performed at 0 °C. The points represents the mean ±SEM of two determinations. The curves are fits to the data using a biexponential function, $Y = f_0 + f_1(1 - e^{-\lambda_1 t}) + f_2(1 - e^{-\lambda_2 t})$ (λ are the observed rate constants and *f* the steady-state phases), which fit the data significantly better than monoexponential functions as judged by F tests. For shark enzyme the fitted rate constants for ATP phosphorylation were (phases given as % in parentheses) 124 ± 13 s^{-1} (38%) and 11.6 ± 0.4 s^{-1} (62%) and for P_i phosphorylation were 0.24 ± 0.05 s^{-1} (57%) and 0.023 ± 0.007 s^{-1} (43%). For pig kidney the fitted rate constants for ATP phosphorylation were 40 ± 5 s^{-1} (47%) and 6.1 ± 0.8 s^{-1} (53%) and for P_i phosphorylation were 0.45 ± 0.07 s^{-1} (53%) and 0.019 ± 0.004 s^{-1} (47%).

RESULTS

Chemical Quench Experiments

Phosphorylation and Dephosphorylation Reactions. Shark rectal or pig renal Na,K-ATPase were phosphorylated either from ATP at [Na^+] = 16 mM or from P_i in the nominal absence of alkali cations. Phosphorylation of both enzyme species from 1 mM ATP followed double-exponential time functions at all temperatures tested. At 0 °C (Figure 1A) the rapid and slow phases were almost equal with observed rate constants of ∼120 and ∼10 s^{-1} for shark enzyme and ∼40 and ∼6 s^{-1} for pig enzyme, as previously found (*19*). Biphasic phosphorylation from ATP has previously been reported (see, e.g., reference (*22*)).

P_i phosphorylation was 400−500 times slower than the ATP phosphorylation. At 0 °C the phosphorylation of shark rectal and pig renal enzyme from 1 mM P_i could be reasonably well fitted with a monoexponential time function ($R^2 > 0.96$) with and identical observed rate constant of 0.084 s^{-1} for both enzyme preparations. However, the phosphorylation was better fitted by double-exponential time functions with observed rate constants of the fast and slow phases as given in the legend to Figure 1B. At 20 °C P_i phosphorylation was better fitted with monoexponential than with double-exponential time functions and an observed rate constant of 0.26 s^{-1} was found for shark enzyme (Table 1).

We cannot say at present why the biphasic behavior in P_i phosphorylation was more pronounced at 0 °C than at higher temperatures; however, extraordinary phosphoenzyme transient kinetics has previously been observed at 0 °C compared to physiological temperatures (*23*). It could indicate that the rate constant for the slower reaction has a temperature coefficient exceeding that of the fast reaction.

For pig kidney enzyme the steady-state EP level after P_i phosphorylation was almost two times higher than that found

Table 1: Comparison of Relative Initial Velocities of Phosphorylations, v_0, of Shark Enzyme Calculated from Double-Exponential Fit to Data from ATP Phosphorylation[a] and from Monoexponential Fits to Phosphorylation Reactions from P_i[b] Measured Either by Rapid Mixing Quenched-Flow or by Rapid Mixing Stopped-Flow RH 421 Fluorescence at 15 and 20 °C

fluorescence			chemical		
ATP (1 mM)		P_i (1 mM)	ATP (1 mM)		P_i (1 mM)
15 °C	20 °C	20 °C	15 °C	20 °C	20 °C
30.7 ± 0.6	72.3 ± 0.7	0.119 ± 0.002	79.6 ± 1.5	168[c]	0.132 ± 0.018

[a] $v_0 = \lambda_1 f_1 + \lambda_2 f_2$, $f_1 + f_2 = 1$. [b] $v_0 = \lambda f$, where f, the relative level of EP, is half of that found from ATP phosphorylations. [c] This value given at 20 °C is calculated from measured values at 0 and 10 °C and an activation energy of 59.8 kJ/mol ($Q_{10} = 2.5$).

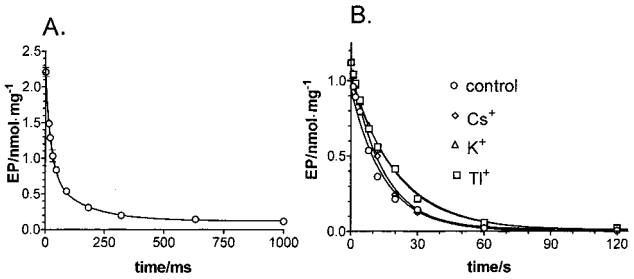

FIGURE 2: K^+-activated dephosphorylation of shark Na,K-ATPase after phosphorylation from either ATP (A) or P_i (B). The enzyme was phosphorylated as described in Figure 1. In the experiments depicted in A, 0.5 mM K^+ (final) was added with the chase solution at 0 time in a rapid mixing quenched-flow setup. In the experiments depicted in B, the dephosphorylation was performed by hand either in the nominal absence of alkali cations (○) or with 5 mM (final) K^+ (△), Tl^+ (□), or Cs^+ (◇) added with the chase solution at 0 time. Note the difference in time scales. The curves are exponential fits to the data. In A a biexponential function, $Y = f_0 + f_1 e^{-\lambda_1 t} + f_2 e^{-\lambda_2 t}$ (λ are the observed rate constants and f the relative steady-state fractions indicated in parentheses), with $\lambda_1 = 38.7 \pm 4.6$ s^{-1} (40%) and $\lambda_2 = 6.3 \pm 0.7$ s^{-1} (60%) was used. In B monoexponential functions fitted the data with the observed rate constants; control, 0.066 ± 0.003 s^{-1}; K^+, 0.049 ± 0.003 s^{-1}; Tl^+, 0.047 ± 0.004 s^{-1}; and Cs^+, 0.070 ± 0.006 s^{-1}. The latter four rate constants are not significantly different by an F test.

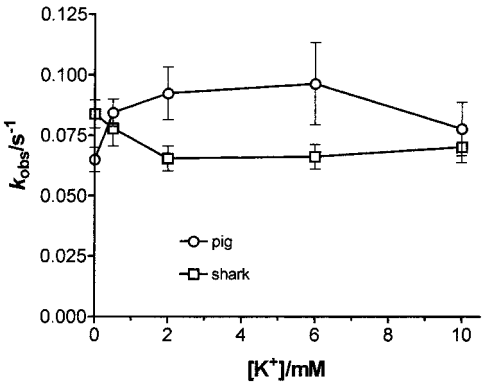

FIGURE 3: Observed rate constants (k_{obs}) for the dephosphorylation of E'_2P as a function of $[K^+]$ in the chase solution for shark enzyme (○) and for pig kidney enzyme (□). The experiments were performed, and the observed rate constants were calculated from monoexponential fits to the data as described in Figure 2B.

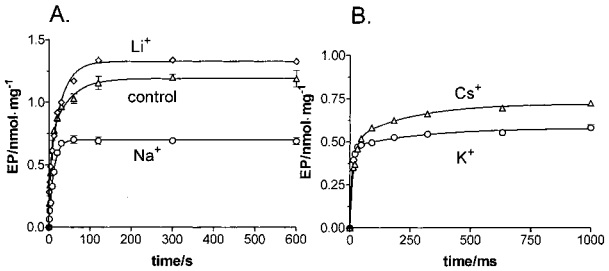

FIGURE 4: Effect of alkali cations on P_i-dependent phosphorylation of shark Na,K-ATPase. All experiments were performed at 0 °C with 4 mM Mg^{2+} and 1 mM P_i and in the absence (control) or in the presence 5 mM alkali cations indicated in the figure. In the experiments shown in B a rapid mixing quenched-flow apparatus was employed. All curves are best exponential fits to the data as evaluated by F tests. Except for Na^+, which could be fitted adequately by a monoexponential time function, the data were better fitted with biexponential time functions. The fitted constants, with absolute values for the slow and rapid phases in parentheses, for the curves in A were the following: in the nominal absence of alkali cations (control), $\lambda_1 = 0.241 \pm 0.049$ s^{-1} (0.68 nmol/mg) and $\lambda_2 = 0.023 \pm 0.007$ s^{-1} (0.51 nmol/mg); with Li^+, $\lambda_1 = 0.91 \pm 0.25$ s^{-1} (0.38 nmol/mg) and $\lambda_2 = 0.037 \pm 0.004$ s^{-1} (0.95 nmol/mg); with Na^+, $\lambda = 0.087 \pm 0.004$ s^{-1} (0. 74 nmol/mg). In B: with K^+, $\lambda_1 = 116.4 \pm 9.3$ s^{-1}(0.47 nmol/mg) and $\lambda_2 = 3.4 \pm 1.1$ s^{-1} (0.11 nmol/mg); and with Cs^+, $\lambda_1 = 64.7 \pm 5.7$ s^{-1} (0.51 nmol/mg) and $\lambda_2 = 4.2 \pm 1.0$ s^{-1} (0.22 nmol/mg).

for shark enzyme and about the same as that for ATP phosphorylation (cf. ref *10*).

In agreement with previous reports (*3*, *19*) the rate of spontaneous dephosphorylation of both E_2P (formed from ATP) and E'_2P (formed from P_i) was identical and calculated from monoexponential fits to be ≈0.07 s^{-1} at 0 °C (Figure 2B) increasing to ≈1.1 s^{-1} at 20 °C (not shown). However, as depicted in Figure 2 there is a tremendous difference in the K^+ sensitivities of these two phosphoforms: Addition of 0.5 mM K^+ increased the dephosphorylation rate of E_2P by a factor of more than 300 (Figure 2A) whereas the dephosphorylation of E'_2P was insensitive to 0.5 mM K^+, as also previously described by Post et al. (*3*, *9*), as well as to 0.5 mM Cs^+ or Tl^+ (Figure 2B). The same results were obtained with pig kidney Na,K-ATPase (not shown). As demonstrated in Figure 3 the dephosphorylation of E'_2P from either shark rectal glands or pig kidney was found to be K^+-insensitive over a substantial K^+ concentration range.

Phosphoenzyme Formed from P_i in the Presence of Alkali Cations. Up to now the described phosphoenzyme was formed from P_i in the nominal absence of alkali cations. In the following, phosphoenzymes formed from P_i in the presence of various alkali cations are characterized. In Figure 4 the P_i phosphorylation of shark enzyme pre-equilibrated with 5 mM of either K^+, Cs^+, Na^+, or Li^+ is shown and compared to enzyme phosphorylated in the absence of alkali cations. K^+ and its congeners Cs^+ (Figure 4B), Rb^+, and Tl^+ (not shown) increased the rate of P_i phosphorylation very significantly, making the estimation of the observed rate constant using a rapid mixing quenched-flow device uncertain even at 0 °C. In contrast, Na^+ and Li^+ were without gross effects on the phosphorylation rate (Figure 4A).

The equilibrium EP level was also dependent on the cation present during phosphorylation. In the presence of 5 mM of either Na^+, Cs^+, or K^+, the steady-state phosphorylation level decreased to about half, whereas in the presence of

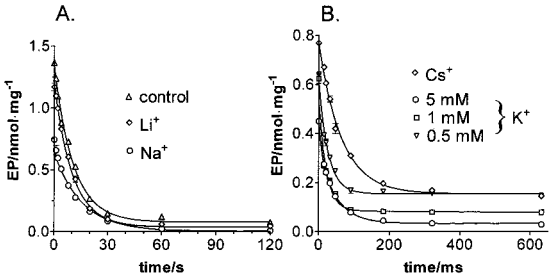

FIGURE 5: Dephosphorylation of phosphoenzyme formed from P_i in the presence of alkali cations. All experiments were performed at 0 °C with shark Na,K-ATPase. The indicated cations were present both during the phosphorylation and the subsequent dephosphorylation at a concentration of 5 mM except for K^+ which was present at concentrations of (▽) 0.5 mM, (□) 1 mM, and (○) 5 mM (B). As seen the steady-state phosphoenzyme level in the presence of 5 mM Cs^+ is identical to the level obtained with 0.5 mM K^+. In the experiments shown in B a rapid mixing quenched-flow apparatus was employed. The dephosphorylations could all be adequately described by monoexponential functions. The fitted observed rate constants were (i) control, 0.091 ± 0.006 s^{-1}; (ii) Na^+, 0.064 ± 0.004 s^{-1}; (iii) Li^+, 0.096 ± 0.005 s^{-1}; (iv) Cs^+, 13.9 ± 1.0 s^{-1}; (v) K^+ 0.5 mM, 33.7 ± 3.0 s^{-1}; (vi) K^+ 1.0 mM, 43.2 ± 3.7 s^{-1}; and (vii) K^+ 5 mM, 20.3 ± 1.8 s^{-1}.

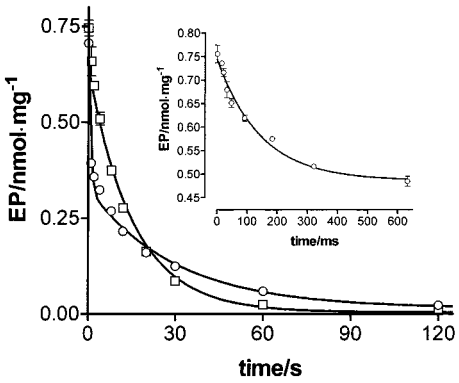

FIGURE 6: K^+-dependent dephosphorylation of phosphoenzyme formed from P_i in the presence of 5 mM Na^+. K^+ (5 mM) (final) was added in the chasing solution (○). The dephosphorylation is clearly biphasic with a rapid phase depicted on an expanded time scale in the inset showing the initial 650 ms of the dephosphorylation in a rapid mixing quenched-flow experiment. The calculated observed rate constants are $\lambda_1 = 6.9 \pm 0.9$ s^{-1} and $\lambda_2 = 0.033 \pm 0.002$ s^{-1}. For comparison the decay of the phosphoenzyme formed under identical conditions but with 5 mM Na^+ present during dephosphorylation is shown (□). In this case the decay could be fitted with a monoexponential time function with an observed rate constant of 0.064 ± 0.004 s^{-1}.

Li^+ it was slightly increased. Similar effects were obtained with pig kidney enzyme except that the steady-state EP level did not decrease when phosphorylation was performed in the presence of 5 mM Na^+ (not shown). In Na,K-ATPase from dog or guinea pig kidney Post et al. (refs *3* and *9* and personal communication) found that low concentrations of Na^+ (<10 mM) abolished completely phosphorylation from P_i. Apart from species differences this is probably due to the use of different [Mg^{2+}] which in the present investigation was found to affect the cation affinity of phosphoenzyme (see Figure 10 and the Discussion).

The effect of the different cations (all in concentrations 5 mM) on the rate of P_i phosphorylation was difficult to compare quantitatively because the phosphorylation reactions were double-exponential time functions where the slow and fast phases and their individual observed rate constants differed for the different cations. Accordingly, the initial rates of phosphorylation (v_0) were compared as explained in Experimental Procedures. Using the fitting parameters in Figure 4, the following series of ion effectiveness in enhancing the rate of phosphorylation from inorganic phosphate was found: Na^+ < control ≤ Li^+ ≪ Cs^+ < K^+ ≅ Rb^+ ≅ Tl^+. The differences in efficiencies of the cations observed at 5 mM concentrations could be caused either by differences in their affinities or by different effects of the bound ions on the maximal rate of phosphorylation, or both.

Dephosphorylation of Phosphoenzyme Formed from P_i in the Presence of Cations. Dephosphorylation experiments were performed with shark Na,K-ATPase with 5 mM either K^+, Cs^+, Na^+, or Li^+, present both during phosphorylation and dephosphorylation, and compared to controls in the absence of alkali cations (Figure 5).

Neither Li^+ nor Na^+ affected significantly the rate of dephosphorylation. The observed rate constants in these experiments were in the same range as for the phosphoenzymes formed and dephosphorylated in the absence of alkali cations, as seen from Figure 5A. The dephosphorylation of the phosphoenzyme formed from P_i in the presence of Na^+ was not accelerated by *N*-methyl hydroxylamine (not shown), contrary to what was observed with the phosphoenzyme formed in the presence of Na^+ and ATP (*10*).

When the phosphoenzyme was formed and dephosphorylated in the presence of 5 mM K^+ or Cs^+ the rate of the dephosphorylation increased dramatically (Figure 5B): the observed rate constant in the presence of 5 mM K^+ calculated for the monoexponential phase of decay increased from 0.07 to about 30 s^{-1}, more than 400-fold. Rb^+ and Tl^+ had effects similar to those of K^+ in accelerating dephosphorylation (not shown). Cs^+ was less efficient and, in contrast to 5 mM K^+, the residual EP level (EP_∞) reached after 300 ms was significantly higher than 0, an effect that was also observed when a lower concentration of K^+ during the phosphorylation reaction was used (Figure 5B). The series of effectiveness in accelerating the rate of dephosphorylation of the phosphoenzyme formed from P_i in the presence of cations was the same as for phosphorylations by P_i: Na^+ < control ≤ Li^+ ≪ Cs^+ < K^+ ≅ Rb^+ ≅ Tl^+. And again the differences in efficiencies of the cations could be due to differences in their affinities, or differences in the maximal rate of dephosphorylation of cation-bound phosphoforms, or both.

The dephosphorylation characteristics were dependent not only on the cation species present during the phosphorylation reaction but also on the cation composition of the dephosphorylation medium. The dephosphorylation of phosphoenzyme formed in the presence of 5 mM K^+ was instantaneously slowed by a dilution of K^+ (to 0.1 mM) in the dephosphorylation medium. In this case k_{obs} was 0.25 s^{-1} (not shown), only a little faster than in experiments where phosphorylation was performed in the absence of K^+ (k_{obs} = 0.07 s^{-1}).

When the enzyme was phosphorylated in the presence of 5 mM Na^+ and then dephosphorylated in the presence of 5 mM K^+ about half of the phosphoenzyme was K^+-sensitive and decayed rapidly ($k_{obs} \sim 7$ s^{-1}) while the other half decayed with a rate similar to that in controls without added alkali cations or with Na^+ alone (Figure 6). In a similar experiment performed with 5 mM Li^+ instead of Na^+ no

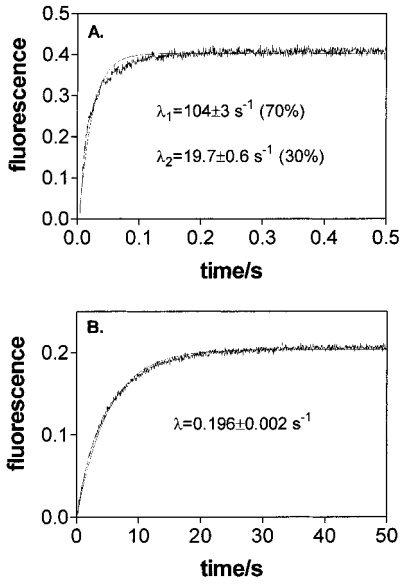

FIGURE 7: Rapid mixing stopped-flow experiments demonstrating the fluorescence response of RH421 to phosphorylation of shark Na,K-ATPase either from ATP in the presence of 16 mM Na^+ (A) or from P_i in the nominal absence of alkali cations (B). In the experiment with ATP one syringe contained the enzyme, RH421 (240 nM), Mg^{2+} (4 mM), imidazole buffer (30 mM), pH 7.5, and 16 mM NaCl. ATP (1.0 mM final) was added from the second syringe containing, in addition, the same medium as the first syringe except for enzyme and RH421. In the experiment with P_i the first syringe contained the enzyme, RH421 (240 nM), Mg^{2+} (4 mM), and Hepes/Mes (10 mM), pH 7.5, and the second syringe 4.45 mM P_i (final). In each experiment 100 μL of solution from each syringe was mixed. The traces are averages of 5−10 experiments consisting of 4000 data points each. All experiments were performed at 20 °C. With ATP the fluorescence change (F) was described by a double-exponential function, $F = f_0 + f_1(1 - e^{-\lambda_1 t}) + f_2(1 - e^{-\lambda_2 t})$. The fit parameters (observed rate constants (λ) and phases (f)) were $\lambda_1 = 104 \pm 3$ s^{-1} (70%) and $\lambda_2 = 19.7 \pm 0.6$ s^{-1} (30%). This corresponds to a relative initial velocity $v_0 = \lambda_1 f_1 + \lambda_2 f_2 = 78.7$ s^{-1}. For P_i phosphorylation a monoexponential time function fit the data adequately with an observed rate constant of 0.196 ± 0.002 s^{-1}.

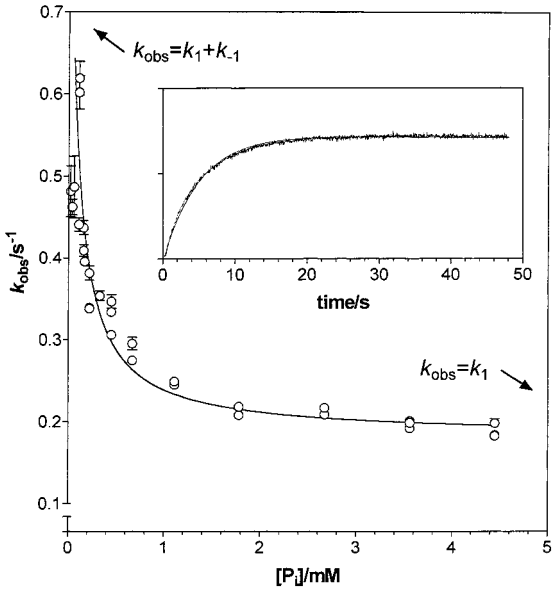

FIGURE 8: The observed rate constants (k_{obs}) for the RH421 fluorescence increase associated with P_i phosphorylation of shark Na,K-ATPase as a function of the P_i concentration. The observed rate constants were estimated from a monoexponential fit to the fluorescence increase of RH421 of shark enzyme phosphorylated by increasing the concentration of inorganic phosphate in the absence of alkali cations. The curve represents a fit of the equation to the data, as explained in the Results:

$$k_{obs} = k_1 + \frac{k_{-1}}{1 + \dfrac{[P_i](1 + k_3/k_{-3})}{K_{Pi}}}$$

In the fit $K_{Pi} = K_{0.5Pi}(1 + k_3/k_{-3})/(1 + k_{-1}/k_1)$ where $K_{0.5Pi} = 330$ μM (*10*) was fixed and $k_3 = k_{-3}$. The calculated rate constants were $k_1 = 0.1872 \pm 0.0001$ s^{-1} and $k_{-1} = 0.948 \pm 0.006$ s^{-1}. The inset shows a model simulation (full curve) to data from a stopped-flow RH421 fluorescence response to P_i phosphorylation at 4.45 mM P_i using Scheme 1 in the Results and the program DYNAFIT (*21*) with the constants $k_1 = 0.18$ s^{-1}, $k_{-1} = 0.95$ s^{-1}, and $K_{0.5Pi} = 330$ μM fixed.

acceleration of dephosphorylation induced by 5 mM K^+ was observed. This was the case for both pig kidney and shark enzyme.

RH421 Fluorescence Experiments

Phosphoenzyme Characterization by RH421 Fluorescence. In the presence of Mg^{2+}, addition of ATP (1 mM and with 16 mM Na^+ in the medium) to shark enzyme induced a rapid fluorescence increase (Figure 7A), whereas addition of P_i (Figure 7B) or vanadate (not shown) resulted in a considerably slower response (cf. ref *10*). As seen from the rapid mixing stopped-flow experiments the fluorescence responses to ATP followed a double-exponential time course, as also found in the chemical quench measurements at 0 °C (Figure 1A). This is also in concert with previous reports using RH421 fluorescence associated with ATP phosphorylation (*24*) whereas the slow phase was not reported in the investigations of Pratap and Robinson (*25*). In 6 experiments with ATP phosphorylation (1.0 mM) of shark enzyme at 20 °C the rapid phase comprised 84% ± 7% with an observed rate constant of 82 ± 2 s^{-1} and a slow phase (18% ± 2%) with observed rate constant of 18 ± 3 s^{-1}. This is significantly slower than found in the rapid mixing quenched-flow experiments (Figure 1A). The same difference in the rates determined from quenched-flow experiments compared to stopped-flow RH421 experiments was found at all temperatures employed, two of which are shown in Table 1, and is most probably caused by the fact that in the chemical quench experiments the acid-stable phosphoenzymes measured include both E_1P and E_2P, whereas in the fluorescence measurements only E_2P is detected as discussed later.

For P_i phosphorylation at 4.45 mM P_i the data could be satisfactorily described by a monoexponential time function with an observed rate constant 0.24 ± 0.006 s^{-1} (means of 8 experiments at 20 °C). This is the same as that found for the observed rate constant in the quenched-flow experiments at 1 mM P_i which is near-saturating (10) (Table 1).

To explore the P_i phosphorylation reaction in further detail we investigated the P_i dependence on the rate of the fluorescence response (Figure 8). As seen the observed rate constant decreased with increasing [P_i] indicating that a rate-determining step (here assumed to represent the $E_1 \rightarrow E_2$ transition) precedes the phosphorylation of E_2 by P_i (Scheme 1):

Scheme 1

$$E_1 \underset{k_{-1}}{\overset{k_1}{\rightleftarrows}} E_2 \underset{k_{-2}}{\overset{k_2}{\rightleftarrows}} E_2{\cdot}P \underset{k_{-3}}{\overset{k_3}{\rightleftarrows}} E'_2P$$

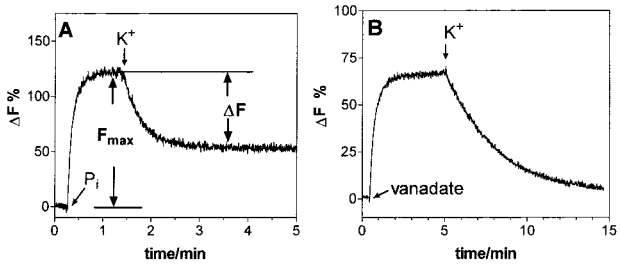

FIGURE 9: Effect of K^+ on the P_i phosphorylation-dependent (A) or vanadylation-dependent (B) RH421 fluorescence level. All experiments were performed with shark enzyme at 20 °C. The $[P_i]$ was 4.45 mM and the vanadate concentration 100 μM. The K^+ concentration was 2 mM for vanadylated enzyme and 1 mM for P_i phosphorylated enzyme. For both experiments the relative decrease in the fluorescence caused by K^+ ($\Delta F/F_{max}$ in %) is calculated as the decrease in fluorescence caused by K^+ addition compared to the maximum fluorescence prior to the addition of K^+.

The analytical expression for the observed rate constant using this scheme can be calculated by the determinantal method (*26*) to give the following:

$$k_{obs} = k_1 + \frac{k_{-1}}{1 + \dfrac{[P_i](1 + k_3/k_{-3})}{K_{Pi}}} \quad (1)$$

where $K_{Pi} = k_{-2}/k_2$ is the dissociation constant for P_i.

As indicated by eq 1 at saturating P_i concentration the observed rate constant approaches k_1 whereas at zero P_i it approaches ($k_1 + k_{-1}$). For shark rectal enzyme it can be assumed that $k_3 = k_{-3}$ since the acid-stable phosphoenzyme level obtained after P_i phosphorylation is half of that found after maximum phosphorylation from ATP (*10*). K_{Pi} is given by the previously determined $K_{0.5Pi} = 330$ μM (*10*) by the following relation:

$$K_{Pi} = K_{0.5Pi} \frac{1 + \dfrac{k_3}{k_{-3}}}{1 + \dfrac{k_{-1}}{k_1}} \quad (2)$$

Fitting of eq 1 to the data shown in Figure 8 gave a $k_1 \approx 0.18$ s^{-1} and a $k_{-1} \approx 0.95$ s^{-1}. The values for k_1 and k_{-1} show that initially the enzyme was mainly in the E_1 form. The calculated dissociation constant for P_i becomes $K_{Pi} \approx 110$ μM for shark rectal Na,K-ATPase. The inset in Figure 8 shows a model simulation using these calculated kinetic constants compared to the stopped-flow RH421 fluorescence response at 4.45 mM P_i.

RH421 Response to Additions of Cations to Phosphoenzyme. When enzyme was phosphorylated from P_i, or reacted with vanadate, subsequent addition of K^+ resulted in a slow decay of the fluorescence to a new equilibrium level (Figure 9). The experiments could not be performed with vanadylated pig kidney enzyme since no fluorescent response accompanied the vanadylation reaction (cf. ref *10*).

The difference in the equilibrium levels of P_i phosphorylation-induced fluorescence (expressed as $\Delta F/F_{max}$, as indicated in Figure 9) with and without addition of K^+ is shown in Figure 10B for shark rectal enzyme and in Figure 11 for pig kidney enzyme as a function of the K^+ concentration. For shark enzyme a sigmoidal dependence with a Hill coefficient >1.5 was found with both K^+ (Figure 10B), Tl^+ (Figure 10A), and Na^+ (Figure 10D). The respective apparent $K_{0.5}$ values were calculated to about 1 mM (K^+), 0.1 mM (Tl^+), and 30 mM (Na^+). For Cs^+ (Figure 10C) a $K_{0.5}$ value of 18.9 mM was found and the Hill coefficient was 0.7. For pig enzyme a hyperbolic dependence of $\Delta F/F_{max}$ on $[K^+]$ was adequate to describe the results, as shown in Figure 11. With all cations studied the apparent affinity was increased by a decrease in the Mg^{2+} concentration in the reaction medium (shown for Na^+ in Figure 10D). This result could in part explain why Post et al. (9) using 1 mM

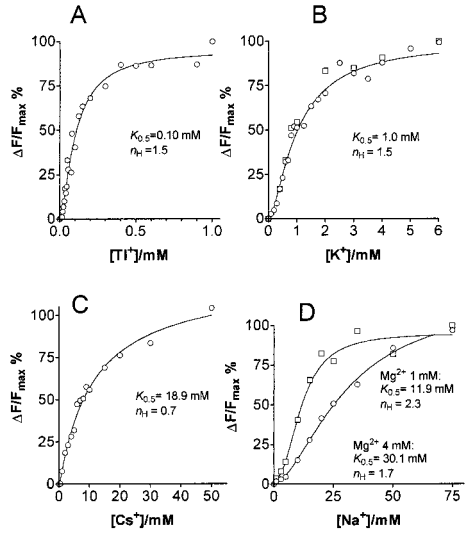

FIGURE 10: Alkali cation-dependent decrease in the equilibrium level of RH421 fluorescence ($\Delta F/F_{max}$, where ΔF and F_{max} were determined as shown in Figure 9) after P_i phosphorylation of shark rectal enzyme. All curves were fitted using the Hill equation with $K_{0.5}$ and Hill coefficients, n_H, indicated on the figure. The points are means ±SEM ($n = 3$). For Na^+ the experiments were performed both at 4 mM Mg^{2+} (○) as with the other cations, and with 1 mM Mg^{2+} (□).

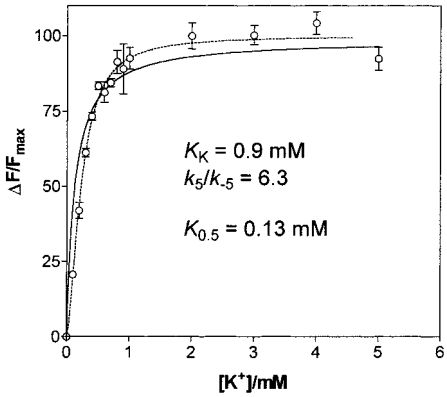

FIGURE 11: K^+-dependent decrease in the equilibrium level of RH421 fluorescence ($\Delta F/F_{max}$ where ΔF and F_{max} were determined as shown in Figure 9) after P_i phosphorylation of pig renal enzyme. The broken curve shows a sigmoidal fit to the data with a Hill coefficient $n_H = 1.7 \pm 0.2$ and $K_{0.5} = 0.23 \pm 0.01$ mM. The continuos curve was drawn using the equation

$$\frac{\Delta F}{F_{max}} = \frac{[K^+]\dfrac{k_5}{k_5 + k_{-5}}}{[K^+] + K_K \dfrac{k_{-5}}{k_5 + k_{-5}}}$$

in which $k_5/k_{-5} = 6.3$ and $K_K = 0.9$ mM as calculated in Figure 12A. The points are means ±SEM ($n = 3$).

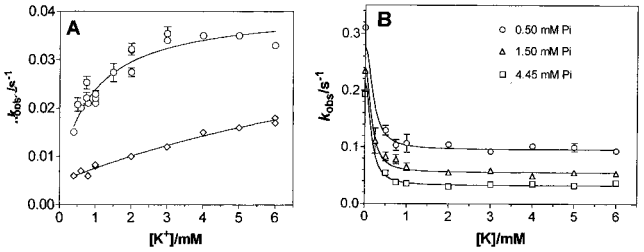

FIGURE 12: Observed rate constants (k_{obs}) for a K^+-dependent decrease in P_i phosphorylation- (or vanadylation-) induced fluorescence (cf. Figure 9) as a function of the K^+ concentration. The observed rate constants were estimated from monoexponential fits to the time course of the K^+-induced decrease in RH421 fluorescence as shown in Figure 9. In A data from two independent experiments are shown for pig kidney enzyme at 4.45 mM P_i (○), and in the lower curve (◇) for vanadylated shark enzyme. These data were fitted with a hyperbolic function: $k_{obs} = k_5[K^+]/(K_K + [K^+]) + k_{-5}$ with the following constants for P_i phosphorylation of pig kidney enzyme: $k_5 = 0.035 \pm 0.004$ s^{-1} and $k_{-5} = 0.006 \pm 0.004$ s^{-1}; and a dissociation constant for K^+, $K_K = 0.9 \pm 0.5$ mM. For vanadylated shark enzyme the following constants were obtained: $k_5 = 0.043 \pm 0.03$ s^{-1}, $k_{-5} = 0.0047 \pm 0.0006$ s^{-1}, and $K_K \approx 14$ mM. B shows the observed rate constant for shark enzyme as a function of $[K^+]$ at three different P_i concentrations (0.5, 1.5, and 4.45 mM). The points on the ordinate are read from the curve given in Figure 8. The curves are computed according to the equation

$$k_{obs} = \frac{k_{-1}}{1 + \dfrac{[P_i](1 + k_3/k_{-3})}{K_{Pi}}} + \frac{k_1}{1 + \left(\dfrac{[K^+]}{K_{0.5K}}\right)^2}$$

as given in the Results. In the fits, k_1 and k_{-1} values calculated from Figure 8 were fixed at 0.18 and 0.95 s^{-1}, respectively. $K_{Pi} = K_{0.5Pi}(1 + k_3/k_{-3})/(1 + k_{-1}/k_1)$ where $K_{0.5\ Pi}$ 330 μM (*10*) was fixed and $k_3 = k_{-3}$. For 0.5 mM P_i, $K_{0.5Pi}$ and $K_{0.5K}$ are found to 352 ± 10 μM and 0.21 ± 0.03 mM; for 1.5 mM P_i, 581 ± 23 μM and 0.17 ± 0.02 mM; and for P_i 4.45 mM, 986 ± 32 μM and 0.16 ± 0.02 mM.

$MgCl_2$ found complete inhibition of P_i phosphorylation by Na^+ at concentrations much lower than those observed in the present paper, where the experiments were performed with 4 mM Mg^{2+}.

In Figure 12A the observed rate constants for the K^+-induced decay of the fluorescence (k_{obs}) of phosphorylated pig renal enzyme and vanadylated shark enzyme are shown. In all cases k_{obs} increased with increasing $[K^+]$. In Figure 12B the results of the same experiments are shown for shark rectal enzyme at three different P_i concentrations. As seen, for P_i phosphorylated shark enzyme k_{obs} decreased at increasing K^+ concentrations.

The differences between the two enzyme sources (pig renal and shark rectal enzyme) in response to K^+ could be related to the significant difference in the equilibrium distribution of phosphate(vanadate)-enzyme forms at saturating substrate concentrations in the two enzymes. In the case of P_i phosphorylation of kidney enzyme or vanadylation of the shark enzyme the equilibrium at saturating substrate is heavily poised toward E'_2P or E_2V, respectively (*10*). In this case the increase of k_{obs} at increasing $[K^+]$ must reflect a rapid binding of K^+ directly to E'_2P (step 4 below) or E_2V followed by a slow transformation to nonfluorescent forms (step 5):

Scheme 2

$$E_1 \underset{k_{-1}}{\overset{k_1}{\rightleftarrows}} E_2 \underset{k_{-2}}{\overset{k_2}{\rightleftarrows}} E_2{\cdot}P \underset{k_{-3}}{\overset{k_3}{\rightleftarrows}} E'_2P \underset{k_{-4}}{\overset{k_4}{\rightleftarrows}} E'_2P{\cdot}K \underset{k_{-5}}{\overset{k_5}{\rightleftarrows}} E'_2P\langle K\rangle$$

The intermediate formed in the initial fast reaction with K^+ (here denoted $E'_2P{\cdot}K$) must be a high-fluorescent form since no rapid phase in the decrease of fluorescence was observed after K^+ addition. This step is followed by a slow transition to a nonfluorescent form which could be either the dephosphorylation of the K^+-bound E'_2P form itself or a slow transition to another phosphoform. The species $E'_2P\langle K\rangle$ (the notation $\langle\ \rangle$ is used to indicate a "loosely occluded" cation, for reasons described in the Discussion) must be low-fluorescent as discussed below. In the reaction sequence (Scheme 2) where K^+ binds directly to E'_2P we have not addressed the question of the stoichiometry of K^+ binding since our data are not sufficiently precise at the lower $[K^+]$. However, using the model in Scheme 2 with binding of only one K^+ it is possible to simulate the results given in Figure 12A using the following expression:

$$k_{obs} = \frac{k_5[K^+]}{K_K + [K^+]} + k_{-5} \qquad (3)$$

in which $K_K = k_{-4}/k_4$ is the dissociation constant for K^+. The fit is shown as the curve in Figure 12A and gave a calculated K^+ dissociation constants, $K_k = 0.9$ mM, and the rate constants, $k_5 = 0.035$ s^{-1} and $k_{-5} = 0.006$ s^{-1}. The dissociation constant for K^+ found here is in accordance with the estimated $K_{0.5}$ for the K^+ binding to E'_2P (≈0.13 mM) found from equilibrium measurements of RH421 fluorescence amplitudes in pig kidney enzyme shown in Figure 11 since K_K will be larger than $K_{0.5}$ by a factor of $(1 + k_5/k_{-5}) \approx 7$. Moreover, the relation of $\Delta F/F_{max}$ vs $[K^+]$ in equilibrium measurements could be satisfactorily fitted with the model given in Scheme 2 using the k_5, k_{-5}, and K_K constants calculated from the stopped-flow RH421 experiment (Figure 12 A) as shown by the continuos curve in Figure 11, although the better sigmoidal fit indicated by the broken curve could be taken to indicate the binding of two K^+ rather than one. The relation between ΔF and $[K^+]$ for binding of one K^+ using Scheme 2 is given by (*27*):

$$\frac{\Delta F}{F_{max}} = \frac{[K^+]\dfrac{k_5}{k_5 + k_{-5}}}{[K^+] + K_K\dfrac{k_{-5}}{k_5 + k_{-5}}} \qquad (4)$$

Vanadylated shark rectal enzyme using the same Scheme 2 for binding of one K^+ to E_2V gave a dissociation constant of ≈14 mM (lower curve in Figure 12 A).

With shark enzyme k_{obs} for the fluorescence decrease after K^+ addition to P_i phosphorylated shark enzyme decreased at increasing $[K^+]$ (Figure 12B). This indicates that it is not induced by K^+ binding to E'_2P (which would result in a hyperbolic increase of k_{obs} vs $[K^+]$ as with pig renal enzyme). Instead, K^+ must preferentially react with some other intermediates, like E_1, shifting the equilibrium away from the high-fluorescent E'_2P form. This is in accordance with an E'_2P level of only 50% of the maximum sites at saturating P_i in shark enzyme showing the existence of substantial dephosphoenzyme species here compared to pig kidney enzyme. The reaction is demonstrated in Scheme 3 below:

Scheme 3

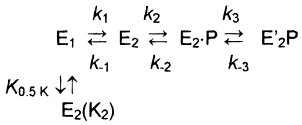

In this scheme binding of two K^+ is indicated as usually presumed. When it is assumed that the $E_2 \rightleftarrows E_1$ transition step is rate-determining, k_{obs} for the K^+ effect on fluorescence can be calculated by the determinantal method (*26*) as the following:

$$k_{obs} = \frac{k_{-1}}{1 + \dfrac{[P_i](1 + k_3/k_{-3})}{K_{Pi}}} + \frac{k_1}{1 + \left(\dfrac{[K^+]}{K_{0.5K}}\right)^2} \qquad (5)$$

in which $K_{0.5K}$ is the apparent constant of half-saturation for the binding of 2 K^+ to E_1.

Equation 5 predicts that, for $[K^+] \rightarrow 0$,

$$k_{obs} \rightarrow \frac{k_{-1}}{1 + \dfrac{[P_i](1 + k_3/k_{-3})}{K_{Pi}}} + k_1$$

in accordance with eq 1 and, for $[K^+] \rightarrow \infty$,

$$k_{obs} \rightarrow \frac{k_{-1}}{1 + \dfrac{[P_i](1 + k_3/k_{-3})}{K_{Pi}}}$$

The latter anticipates that at saturating $[K^+]$, k_{obs} should decrease with increasing $[P_i]$. As seen from Figure 12B, this is confirmed experimentally.

In Figure 12B the data for k_{obs} are shown for three different concentrations of P_i and are each fitted with eq 5 using values for k_1 (0.18 s^{-1}) and k_{-1} (0.95 s^{-1}) identical to those found previously from the data given in Figure 8. Moreover, $k_3 = k_{-3}$ and $K_{Pi} = K_{0.5Pi}(1 + k_3/k_{-3})/(1 + k_{-1}/k_1)$ as described before for eq 1. In principle, the calculated $K_{0.5Pi}$ should be 330 μM (*10*) for all three curves and $K_{0.5K}$ should also be identical in the three fits. $K_{0.5K}$ varied insignificantly between 0.16 and 0.21 mM, whereas $K_{0.5Pi}$ increased from 352 to 986 μM when the $[P_i]$ concentration increased from 0.5 to 4.45 mM (see legend to Figure 12B). This variation in $K_{0.5Pi}$ calculated from the three fits in Figure 12B is probably caused by the use of the total $[P_i]$ in the calculations rather than the concentration of its Mg complex which is presumably the true substrate. In accordance with this the closest fit of $K_{0.5Pi}$ to the expected value of 330 μM is derived at the lowest $[P_i]$ where the total P_i concentration is nearly equal to the concentration of its Mg complex. The $K_{0.5K}$ of about 0.2 mM evaluated from the relation of k_{obs} vs $[K^+]$ in stopped-flow RH421 fluorescence measurements in the presence of 4.45 mM P_i (Figure 12B) matched the $K_{0.5}$ of about 1 mM estimated from the fluorescence amplitude vs $[K^+]$ in equilibrium RH421 measurements at 4.45 mM P_i given in Figure 10B. The $K_{0.5}$ found in equilibrium measurements will be larger than the $K_{0.5K}$ from transient measurements by a factor of $\{1 + (1 + [Pi](1 + k_{-3}/k_3)/K_{Pi})k_1/k_{-1}\}^{1/2}$ which with the present rate constants is about 4.

Therefore, with both pig renal and shark rectal enzymes the final fluorescence level after K^+ addition can be explained as being due to a decrease in the equilibrium fraction of the high-fluorescent E'_2P form. The kinetics, however, are different: with pig Na,K-ATPase the fluorescence decreases in response to K^+ binding directly to E'_2P with a dissociation constant, K_K, of about 0.9 mM assuming binding of one K^+ (Figures 11 and 12A). With shark Na,K-ATPase the fluorescence decrease reflects mainly binding of K^+ to E_1 followed by the occlusion of K^+ with a $K_{0.5K}$ of about 0.2 mM (Figures 10B and 12B).

RH421 Response to Phosphorylation in the Presence of Alkali Cations. Addition of P_i to kidney or shark enzymes pre-equilibrated with alkali ions resulted in a fluorescence increase with an amplitude ($\Delta F/F_{max}$) which varied with the concentration of the cation as indicated in Figure 10: at 1 mM K^+ only 50% of the fluorescence response in the absence of cations is obtained, whereas the fluorescence response is unchanged with 1 mM Cs^+ or Na^+, but completely abolished with 1 mM Tl^+.

DISCUSSION

In the present investigation biochemical and fluorescent methods were applied to study the formation and the properties of phosphoenzymes formed from inorganic phosphate in the absence and in the presence of alkali cations and compared with the properties of phosphoenzymes formed from ATP. The study was performed with Na,K-ATPase from two sources, pig kidney and shark rectal glands, and the fluorescence measurements were performed with the membrane-embedded styryl dye RH421. The model used to analyze the response to the P_i phosphorylation and the effects of alkali cations is summarized in Scheme 4:

Scheme 4

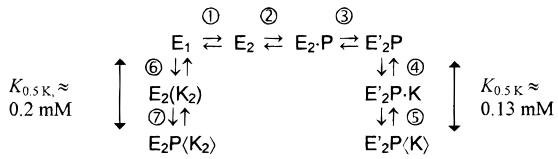

Phosphorylation from P_i in the Absence of Alkali Cations. Chemical and Fluorescence Measurements. For phosphorylation from P_i there is now ample evidence that the increase in RH421 fluorescence (Figure 7) reflects the formation of the acid-stable phosphoenzyme, E'_2P (10). For ATP phosphorylation it has previously been demonstrated that RH421 fluorescence detects the formation of K^+-sensitive E_2P but not of ADP-sensitive E_1P. This was shown by experiments using enzyme treated with chymotrypsin (*28*, *29*) which blocks the $E_1P \rightleftarrows E_2P$ transition or with oligomycin (25) which also stabilizes E_1P. In both cases the RH421 fluorescence response to ATP addition was either completely or partially inhibited. This also explains the difference in shark enzyme between the observed rates of ATP phosphorylation evaluated from chemical experiments, where the total amount of phosphoenzyme ($E_1P + E_2P$) is measured, and RH421 fluorescence experiments, which only detect E_2P (Table 1), assuming that the $E_1P \rightleftarrows E_2P$ transition is the rate-determining step. In contrast to the present results with shark enzyme the phosphorylation reaction in mammal preparations has been found to be rate-determining, at least at 24 °C (24).

Table 2: Assignment of Rate Constants and Cation Affinities to the Reaction Schemes 2 and 4 of Shark Rectal and Pig Kidney Na,K-ATPase Using RH421 Fluorescence

reaction	calculated value	reference
	Shark Enzyme	
$E_1 \rightleftarrows E_2$	$k_1 \sim 0.18\ s^{-1}$	Figure 8
	$k_{-1} \sim 0.95\ s^{-1}$	
$E_2 + P_i \rightleftarrows E_2{\cdot}P$	$K_{Pi} \sim 110\ \mu M$	Figure 8
$E_1 \rightleftarrows E_2(K_2)$	$K_{0.5\,K} \sim 0.2$ mM	Figures 10B and 12B
	Pig Kidney Enzyme	
$E'_2P \rightleftarrows E'_2PK$	$K_K \sim 0.9$ mM	Figures 11 and 12A
$E'_2PK \rightleftarrows E'_2P\langle K\rangle$	$k_5 \sim 0.04\ s^{-1}$	Figure 12A
	$k_{-5} \sim 0.006\ s^{-1}$	

In experiments with shark rectal Na,K-ATPase, where RH421 is used to detect the P_i phosphorylation reaction in the absence of alkali cations, the observed rate constant decreased with increasing [P_i] (Figure 8), which indicates that a slow transition of E_1 to E_2 (step 1 in Scheme 4) precedes a fast reaction with P_i (step 2 in Scheme 4). The analysis of the dependency of the observed rate constants determined from stopped-flow RH421 fluorescence on [P_i] (see Results) allows the estimation of the dissociation constant for P_i ($K_{Pi} \approx 110\ \mu M$) as well as the rate constants for the $E_1 \rightleftarrows E_2$ transition (Figure 8 and Table 2). The latter indicates that the E_1/E_2 ratio before phosphorylation is about 5/1 at the experimental conditions used. The predominance of E_1 over E_2 is in accordance with previous results by Fedosova and Klodos (*30*) using pig kidney enzyme at comparable buffer conditions.

Apell et al. (*11*), using rabbit kidney Na,K-ATPase and caged P_i, observed biphasic responses of RH421 to P_i phosphorylation in the absence of cations. They analyzed the data using a simple model $E_1 \rightleftarrows E_2 + P_i \rightleftarrows E_2$-P and ascribed the fast phase to the phosphorylation of the E_2 form of the enzyme, since the rate for this phase was a linear function of [P_i] up to 60 μM. The slow phase was assigned to the $E_1 \rightleftarrows E_2$ transition, and from the ratio of the slow and fast phases, they evaluated the ratio of $E_1/E_2 = {}^1/_2$. In the present experiments the P_i phosphorylation, measured with both ^{32}P and RH421 at 20 °C, was monoexponential, in accordance with the predominant presence of E_1. At present we do not know if the discrepancy between our data and those of Apell et al. (*11*) is due to the use of enzymes from different sources, or experimental conditions, or to the use of caged substrate.

Effects of K^+ and its Congeners on E'_2P. The dephosphorylation rate of phosphoenzyme formed from P_i in the absence of cations is, as described earlier by Post et al. (*3*), virtually independent of the presence of K^+. This is in agreement with the results of the present investigation, where the dephosphorylation of ^{32}P-E was not affected by [K^+] ≤ 10 mM (Figures 2B and 3).

When K^+, 6 mM or less, was added to phosphoenzyme formed from P_i a slow decrease in the RH421 fluorescence was observed with both pig kidney and shark rectal gland enzymes (Figure 9). The measured $K_{0.5}$ for K^+ from equilibrium experiments of the $\Delta F/F_{max}$ vs [K^+] relation (Figures 10 and 11) was in agreement with transient measurements of k_{obs} for the fluorescence decrease vs [K^+] (Figure 12), assuming that in shark the K^+ effects are exerted through binding to the dephosphoform (E_1) whereas in pig enzyme it is through binding to the phosphoenzyme (E'_2P).

The apparent affinities for K^+ and its congeners found here are within the same range as that found in other investigations. Nagel et al. (*31*) found $K_{0.5}$ for K^+ to be 0.7 mM in experiments with pig kidney membranes adsorbed to planar bilayer membranes. Gropp et al. (*32*) found between 2 and 5 mM for the intrinsic dissociation constant of K^+ to phosphoenzyme produced by ATP (E_2P) using reconstituted shark rectal Na,K-ATPase adsorbed to planar bilayer membranes. Gache et al. (*33*), using axonal Na,K-ATPase, found a $K_{0.5}$ for K^+ of 0.8 mM much the same as that for Rb^+, whereas the affinity was higher for Tl^+ (0.25 mM) and much lower for Cs^+ (7 mM).

It should be noted that for any given cation concentration (up to 5 mM) the decrease in the level of fluorescence was more pronounced than could be accounted for by the decreased level of acid-stable phosphoenzyme measured with $^{32}P_i$ in the presence of cations (compare Figures 9, 10, and 11 with Figure 4 and the initial values in Figure 5). This indicates that the cation-bound acid-stable phosphoenzyme species (or cation-bound vanadylated enzyme species) are low or nonfluorescent in accord with the notion that the decrease in the fluorescence is due to the slow establishment of a new equilibrium within the pool of acid-stabile phosphoenzyme forms, or vanadylated enzyme species, between species with and without bound cations.

Properties of the Phosphoenzyme Formed from P_i in the Presence of Alkali Cations. Chemical Measurements. When the enzyme is phosphorylated by P_i in the presence of K^+ or its congeners the measured equilibrium level of acid-stable phosphoenzymes is lower than that found in the absence of the cations and the phosphorylation kinetics become biphasic (Figure 4). In the presence of K^+ the observed rate constant for the rapid phase (~120 s^{-1}) is more than 1000 times faster than in the phosphorylation reaction without K^+ (k_{obs} ~0.09 s^{-1}), both measured at 1 mM P_i and 0 °C. The effect is probably mediated by an acceleration of the K^+ occlusion step, $E_1{\cdot}K_2 \rightarrow E_2(K_2)$ (*34*, *35*). This observed rate constant for phosphorylation is of the same order of magnitude as that suggested by Apell et al. (*11*) for P_i phosphorylation of the E_2 form, taking into account that our experiments are performed at 0 °C while the studies of Apell et al. (*11*) were done at 20 °C (assuming a Q_{10} of 2.5 the rate constant suggested by Apell et al. (*11*), $1.5 \times 10^5\ M^{-1}\ s^{-1}$, corresponds to ~110 s^{-1} at 0 °C and 4.45 mM P_i). The phosphorylation in the two cases leads, however, to formation of different phosphoforms, a K^+-insensitive E'_2P form in the absence of cations and a K^+-sensitive $E_2P\langle K_2\rangle$ form in the presence of K^+ or its congeners, Figure 5B. The last form dephosphorylates at 5 mM K^+ with an observed rate constant between 20 and 40 s^{-1}, compared to an observed rate constant of ~0.07 s^{-1} for the E'_2P form, both measured at 0 °C. With 5 mM K^+ present before and during P_i phosphorylation the equilibrium is poised toward $E_2(K_2)$ and thus $E_2P\langle K_2\rangle$ is the only phosphoenzyme formed as shown by the absence of the slow phase in the subsequent dephosphorylation (Figure 5B, lower curve). The fact that the initial velocity of dephosphorylation of the phosphoenzyme formed and dephosphorylated in the presence of Cs^+ is about three times lower than in the presence of K^+ shows that the phosphoenzyme form which dephosphorylates is the cation-bound phosphoenzyme and not the empty phosphoenzyme.

The rapid dephosphorylation of the K^+-sensitive phosphoenzyme was instantaneously slowed by K^+ dilution in the dephosphorylation medium, indicating that phosphorylation leads to a rapid deocclusion of K^+; this is the reason we indicate the form by $E_2P\langle K_2\rangle$ to emphasize that K^+ is not occluded as in the $E_2(K_2)$ form. The fact that the apparent rate constant of dephosphorylation even at very low [K^+] (0.1 mM) is about 4 times higher than the dephosphorylation of E'_2P could indicate either that only one K^+ leaves the cation-binding site and/or that the rate of K^+ rebinding is very high compared to the transition rate of K^+-sensitive E_2P to K^+-insensitive E'_2P. There is experimental evidence in favor of a phosphoform with only one bound K^+ from studies of Forbush (*36*), who has shown that at low K^+ concentration the release of one of the two occluded K^+ is very fast, whereas the second K^+ leaves the cation-binding site slowly.

When the phosphoenzyme was formed at lower [K^+] or with some of the K^+ congeners, a substantial fraction did not decay within the millisecond time range (Figure 5B). This fraction appears to represent the slowly decaying cation-free E'_2P form, and thus, the amount of the slowly dephosphorylating phase could reflect the cations' affinity toward the enzyme and their ability to promote formation of $E_2(X_2)$ and the subsequently formed K^+-sensitive phosphoform. With 5 mM Cs^+ the level reached after 240 ms is equal to the level reached with 0.5 mM K^+ indicating an affinity 10 times lower of Cs^+ than of K^+ for E_1 (Figure 5B, upper curve) in accordance with the apparent affinities measured by the fluorescence method and depicted in Figure 10.

Contrary to K^+ and its congeners, 5 mM Na^+ or Li^+ was able neither to increase the rate of phosphorylation nor to stimulate the dephosphorylation. While the lack of effect of Li^+ could be due to a rather low affinity of the enzyme toward Li^+ (~100 mM, not shown) and therefore the predominance of E'_2P even in the presence of Li^+, the effect of Na^+ was more complex. Although dephosphorylation in the presence of Na^+ was slow, it increased significantly when Na^+ in the dephosphorylation medium was replaced with K^+, indicating that Na^+ could prevent the formation of K^+-insensitive E'_2P. However, even with 5 mM K^+ in the dephosphorylation medium the dephosphorylation rate of the Na^+-induced phosphoform was 4 times lower than for the phosphoenzyme induced by K^+. It has to be stressed that the phosphoenzymes formed in the presence of Na^+ and P_i and those formed in the presence of Na^+, Mg^{2+}, and ATP are kinetically different. They vary not only with respect to the rate of K^+-induced dephosphorylation (Figures 2 and 6) but also in their reaction with *N*-methyl hydroxylamine, which accelerated the dephosphorylation of the phosphoenzyme formed from ATP by a factor of 400 (*10*) but had no effect on the dephosphorylation of the phosphoenzyme formed from P_i in the presence of Na^+.

Model. The described interactions between the cation-binding sites and the substrate-binding site are summarized in the model presented in Figure 13.

(I) In the absence of cations phosphorylation by inorganic phosphate (steps 1 → 5 in Scheme 4) results in the formation of a phosphoenzyme (Figure 13A) characterized by the following: (1) An inaccessible acyl-phosphate bond, that is, the substrate-binding site in E'_2P is in a "closed" conformation as shown by a low rate of hydrolysis of the acyl-phosphate bond and by the absence of effect of *N*-methyl hydroxylamine (*10*). (2) An ability to bind at least 1 K^+ (RH421 fluorescence experiments) followed by a slow transformation to a low-fluorescent form which we denoted $E'_2P\langle K\rangle$ to make the signature comparable to that used for the species formed from P_i phosphorylation of enzyme preincubated with K^+ (see II below). K^+ binding to E'_2P does not induce an "open" conformation of the substrate site. This is shown by only a slight increase in the dephosphorylation rate at high K^+ concentrations (present paper and Post (personal communication)), but the maximal rate of this dephosphorylation was much lower than that observed for the phosphoenzyme formed and dephosphorylated in the presence of 5 mM K^+.

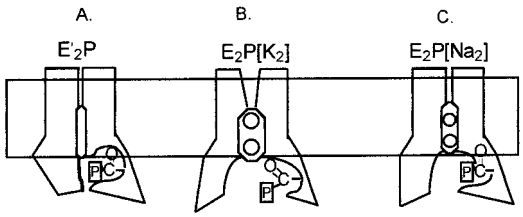

FIGURE 13: A sketch showing the proposed two subconformations of E_2P. The figure illustrates how the cation occupancy in the occlusion pocket could determine the accessibility or the reactivity of the acyl-phosphate bond. With two K^+ occluded the acyl-phosphate bond is very reactive and easily reacts with hydroxylamine or water. When Na^+ is occluded instead of K^+ the acyl-phosphate bond is partially shielded, and without cations in the occlusion pocket, the access to the acyl-phosphate bond is very restricted.

(II) In the presence of alkali cations (Figure 13B) like K^+ and its congeners (Tl^+, Rb^+, and Cs^+ indicated as X^+) in the phosphorylation medium the cations become occluded *prior* to phosphorylation (steps 6 and 7 in Scheme 4). The occlusion affects the subsequent phosphorylation inducing an "open" conformation of the phosphorylation site, as shown by a very high rate of the phosphorylation. This phosphoenzyme dephosphorylates very rapidly in the presence of K^+ (or its congeners X^+) and is, therefore, denoted as an E_2P conformation. Moreover, the phosphorylation of the K^+-bound enzyme leads to an opening of the cation-binding site (indicated with $\langle\ \rangle$), as shown by an instantaneous decrease of the dephosphorylation rate upon K^+ dilution (not shown).

(III) Na^+ has a dual effect. It shifts the equilibrium toward E_1, thus competing with P_i for the enzyme. Although both the phosphoenzyme formation and the dephosphorylation are slow in the presence of Na^+, the phosphoenzyme is, however, sensitive to K^+. This indicates an "open" conformation of the cation-binding sites where at least one Na^+ can exchange rapidly for K^+ (Figure 13C). Moreover, the fast dephosphorylation in the presence of K^+ suggests that Na^+ has a K^+-like effect: being occluded *prior* to the formation of E_2P it prevents the formation of K^+-insensitive E'_2P. Such a K^+-like effect of Na^+ has previously been suggested for Na^+: Na^+ exchange associated with ATP hydrolysis (*37*) and for the phosphorylation of the enzyme in the absence of K^+ (*38*). The fact that K^+ binding increased the rate constant of dephosphorylation to a value which is 4 times lower than for the enzyme phosphorylated and dephosphorylated in the presence of K^+ alone indicates that the substrate-binding site of the phosphoenzyme formed in the presence of Na^+ is only partially "open". This notion is supported by a lack of *N*-methyl hydroxylamine (100 mM) effect on the decay of

this form, which could suggest that the phosphate bond of this form is "shielded", unlike that of E_2P formed from ATP or of $E_2P\langle K_2\rangle$ formed from P_i in the presence of K^+ (or its congeners).

The difference observed in the reactivity in P_i phosphorylation/dephosphorylation (Figures 4 and 5) toward a series of alkali cations could indicate that binding of the cations affects the structure of the substrate site by some allosteric mechanism. Alternatively, the cations could have different abilities to increase the water disorder near the substrate site, thereby destabilizing the acyl-phosphate bond to a different degree. The effective ions all have "structure-breaking entropies" around 14 cal deg^{-1} mol^{-1}, whereas for the ineffective Li^+ and Na^+ it is much smaller, 1.1 and 4.0 cal deg^{-1} mol^{-1}, respectively (*39*).

ACKNOWLEDGMENT

Hanne Zakarias, Ann-Dorit Andersen, Henriette Rugholm Petersen, and Angielina Damgaard are gratefully acknowledged for excellent technical assistance. Bliss Forbush III, with whom the study on RH dyes began, is gratefully acknowledged for stimulating discussions. We would like to thank Drs. R. L. Post and R. J. Clarke for critical reading of the manuscript and for stimulating discussions.

REFERENCES

1. Sen, A. K., Tobin, T., and Post, R. L. (1969) *J. Biol. Chem. 244*, 6596−6604.
2. Siegel, G. J., Koval, G. J., and Albers, R. W. (1969) *J. Biol. Chem. 244*, 3264−3269.
3. Post, R. L., Toda, G., and Rogers, F. N. (1975) *J. Biol. Chem. 250*, 691−701.
4. Robinson, J. D., and Flashner, M. S. (1979) *Biochim. Biophys. Acta 549*, 145−176.
5. Bonting, S. L., Schuurmans Stekhoven, F. M. A. H., Swarts, H. G. P., and De Pont, J. J. H. H. M. (1979) in *Na, K.-ATPase Structure and Kinetics* (Skou, J. C., and Nørby, J. G., Eds.) pp 317−330, Academic Press, London.
6. Schuurmans Stekhoven, F. M. A. S., Swarts, H. G. P., De Pont, J. J. H. H. M., and Bonting, S. L. (1980) *Biochim. Biophys. Acta 649*, 533−540.
7. Sontheimer, G. M., Kalbitzer, H. R., and Hasselbach, W. (1987) *Biochemistry 26*, 2701−2706.
8. Berberián, G., and Beaugé, L. (1991) *Biochim. Biophys. Acta 1063*, 217−225.
9. Post, R. L., Taniguchi, K., and Toda, G. (1974) *Ann. N.Y. Acad. Sci. 242*, 80−90.
10. Fedosova. N. U., Cornelius, F., and Klodos, I (1998) *Biochemistry 37*, 13634−13642.
11. Apell, H.-J., Roudna, M., Corrie, J. E., and Trentham, D. R. (1996) *Biochemistry 35*, 10922−10930.
12. Cornelius, F., Fedosova, N. U., and Klodos, I. (1997) *Ann. N.Y. Acad. Sci. 834*, 390−393.
13. Skou, J. C., and Esmann, M. (1979) *Biochim. Biophys. Acta 567*, 436−444.
14. Jørgensen, P. L. (1974) *Biochim. Biophys. Acta 356*, 36−52.
15. Jensen, J., Nørby, J. G., and Ottolenghi, P. (1984) *J. Physiol. (London) 346*, 219−241.
16. Ottolenghi, P. (1975) *Biochem. J. 151*, 61−66.
17. Lowry, O. H., Rosebrough, N. J., Farr, A. L., and Randall, R. J. (1951) *J. Biol. Chem. 193*, 265−275.
18. Jensen, J., and Ottolenghi, P. (1983) *Biochim. Biophys. Acta 731*, 282−289.
19. Cornelius, F. (1995) *Biochim. Biophys. Acta 1235*, 197−204.
20. Shipley, R. A., and Clark, R. E. (1972) *Tracer Methods for in vivo Kinetics*, Academic Press, New York.
21. Kuzmic, P. (1996) *Anal. Biochem. 237*, 260−273.
22. Froehlich, J. P., and Fendler, K. (1991) in *The Sodium Pump: Structure, Mechanism, and Regulation* (Kaplan, J. H., and De Weer, P., Eds.) pp 227−247, The Rockefeller University Press, New York.
23. Klodos, I., Post, R. L., and Forbush, B., III (1994) *J. Biol. Chem. 269*, 1734−1743.
24. Kane, D. J., Fendler, K., Grell, E., Bamberg, E., Taniguchi, K., Froehlich, J. P., and Clarke, R. J. (1997) *Biochemistry 36*, 13406−13420.
25. Pratap, P. R., and Robinson, J. D. (1993) *Biochim. Biophys. Acta 1151*, 89−98
26. Hammes, G. G., and Schimmel, P. R. (1967) *J. Phys. Chem. 71*, 917−923.
27. Smirnova, I. N., and Faller, L. D. (1993) *J. Biol. Chem. 268*, 16120−16123.
28. Stürmer, W., Bühler, R., Apell, H.-J., and Läuger, P. (1991) *J. Membr. Biol. 121*, 163−176.
29. Klodos, I. (1994) In *The Sodium Pump* (Bamberg, E., and Schoner, W., Eds.) pp 517−528, Steinkopff, Darmstadt.
30. Fedosova. N. U., and Klodos, I. (1994) In *The Sodium Pump* (Bamberg. E., and Schoner, W. Eds.) pp 561−564, Steinkopff, Darmstadt.
31. Nagel, G., Fendler, K., Grell, E., and Bamberg, E. (1987) *Biochim. Biophys. Acta 901*, 239−249.
32. Gropp, T., Cornelius, F., and Fendler, K. (1998) *Biochim. Biophys. Acta 1368*, 184−200
33. Gache, C., Rossi, B., Leone, F. A., and Lazdunski, M. (1979) in *Na, K-ATPase Structure and Kinetics* (Skou, J. C., and Nørby, J. G., Eds.) pp 301−314, Academic Press, London.
34. Karlish, S. J. D., Yates, D. W., and Glynn, I. M. (1978a) *Biochim. Biophys. Acta 252*, 230−251
35. Karlish, S. J. D., Yates, D. W., and Glynn, I. M. (1978b) *Biochim. Biophys. Acta 252*, 252−264.
36. Forbush, B., III (1987) *J. Biol. Chem. 262*, 11116−11127.
37. Cornelius, F., and Skou, J. C. (1985) *Biochim. Biophys. Acta 818*, 211−221.
38. Klodos, I., Fedosova, N. U., and Plesner, I. (1995) *J. Biol. Chem. 270*, 4244−4254.
39. Frank, H. S., and Evans, M. W. (1945) *J. Chem. Phys. 13*, 507.

BI981571V